Available online at www.sciencedirect.com
ScienceDirect
Polymer 48 (2007) 4704–4714
polymer
www.elsevier.com/locate/polymer

Pyridylphosphine ligands for iron-based atom transfer radical polymerization of methyl methacrylate and styrene

Zhigang Xue [a], Bae Wook Lee [a], Seok Kyun Noh [a,*], Won Seok Lyoo [b]

[a] School of Display and Chemical Engineering, Yeungnam University, 214-1 Dae-dong, Gyeongsan, Gyeongbuk 712-749, Republic of Korea
[b] School of Textiles, Yeungnam University, 214-1 Dae-dong, Gyeongsan, Gyeongbuk 712-749, Republic of Korea

Received 6 April 2007; received in revised form 7 June 2007; accepted 8 June 2007
Available online 15 June 2007

Abstract

Two pyridylphosphine ligands, 2-(diphenylphosphino)pyridine (DPPP) and 2-[(diphenylphosphino)methyl]pyridine (DPPMP), were investigated as complexing ligands in the iron-mediated atom transfer radical polymerization (ATRP) of methyl methacrylate (MMA) and styrene with various initiators and solvents. In studies of their ATRP behavior, the $FeBr_2$/DPPP catalytic system was a more efficient ATRP catalyst for the MMA polymerization than the other complexes studied in this paper. Most of these systems were well controlled with a linear increase in the number-average molecular weights (M_n) vs. conversion and relatively low molecular weight distributions ($M_w/M_n = 1.15-1.3$) being observed throughout the reactions, and the measured molecular weights matched the predicted values with the DPPP ligand. The polymerization rate of MMA attained a maximum at a ratio of ligand to metal of 2:1 in *p*-xylene at 80 °C. The polymerization was faster in polar solvents than in *p*-xylene. The 2-bromopropionitrile (BPN) initiated ATRP of MMA with the FeX_2/DPPP catalytic system (X = Cl, Br) was able to be controlled in *p*-xylene at 80 °C. The polymerization of styrene was able to be controlled using the PECl/$FeCl_2$/DPPP system in DMF at 110 °C.

Keywords: Atom transfer radical polymerization; Pyridylphosphine ligands; Iron halide

1. Introduction

Atom transfer radical polymerization (ATRP) is one of the most versatile controlled/"living" radical polymerization methods that allows for the preparation of polymeric materials with well-defined molecular weights [1–5]. In recent years, ATRP has been extensively investigated. ATRP employs a redox process with transition metal complexes in which a halogen atom is transferred reversibly between the transition metal and the end of the polymer chain. In the ATRP system, several transition metals have been investigated in an attempt to accomplish the living radical polymerization of a wide range of monomers with alkyl halides [6–9] or other initiators [10–13] in different solvents.

The catalyst plays an important role in ATRP and for this purpose, various catalytic systems, such as CuBr/2,2′-bipyridine (bpy) [14,15], FeX_2/PPh_3 [10,16], and $RuCl_2(PPh_3)_3/Al(OiPr)_3$ [17], have been used to control the polymerization of methyl methacrylate and styrene. The key to a successful ATRP is the utilization of a proper catalytic system with high activity and selectivity. Recently, iron salt-based catalysts have attracted particular attention [18,19], owing to their low toxicity, low cost, and biocompatibility.

A suitable ligand can lower the redox potential of the metal and improve both the activity and the controllability of the catalyst. Therefore, designing new ligands that are cheaper and more easily available and show better catalytic behavior has become an important research direction in ATRP. As a result, a variety of ligands have been successfully explored in ATRP, including mono- and disubstituted 2,2′-bipyridine [20], multidentate nitrogen ligands [21,22], triphenylphosphines and trialkylphosphines [10,16], and other ligands [23–26]. Matyjaszewski and Nanda [22,27] made a great deal of effort to determine the relationship between the structure of the ligand and its ability to control the polymerization. Pyridylphosphine ligands (Scheme 1) are applied widely in the

* Corresponding author. Tel.: +82 53 810 2526; fax: +82 53 810 4631.
E-mail address: sknoh@ynu.ac.kr (S.K. Noh).

0032-3861/$ - see front matter © 2007 Elsevier Ltd. All rights reserved.
doi:10.1016/j.polymer.2007.06.019

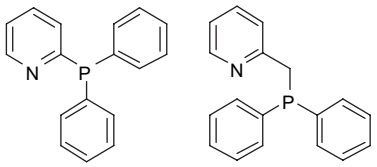

DPPP DPPMP

Scheme 1. The DPPP and DPPMP ligands employed in the polymerization reactions of MMA and styrene.

coordination chemistry of transition metals, owing to the simultaneous presence of the ubiquitous pyridine and phosphine donor groups [28]. DPPP and DPPMP are increasingly used in the synthesis of heterobimetallic or polymetallic compounds. However, bidentate catalyst systems with both phosphorus and nitrogen are rarely studied in ATRP systems. There are no polymerization reactions using CuX/DPPP or CuX/DPPMP catalyst systems because of the difficulty of forming complex. The nickel-mediated living radical polymerization is ongoing to develop the catalyst systems.

In the present study, the polymerizations of MMA and styrene were carried out in the catalyst system, FeX_2/pyridylphosphine. The results showed that the polymerization process is efficient. This system was able to yield poly(methyl methacrylate) (PMMA) and polystyrene (PS) with controlled molecular weights and relatively low polydispersities (PDIs).

2. Experimental section

2.1. Materials

Methyl methacrylate (MMA) (Aldrich, 99%) and styrene (Aldrich, 99%) were passed through a column filled with neutral alumina, dried over CaH_2, distilled under reduced pressure, and stored in a freezer under nitrogen. Tetrahydrofuran (THF) (Fisher, HPLC grade) was freshly distilled from Na/K alloy with benzophenone (Aldrich, 99%) and stored under nitrogen. 2-(Diphenylphosphino)pyridine (DPPP) (Aldrich, 97%), triphenylphosphine (TPP) (Aldrich, 99%), $FeBr_2$ (Aldrich, 98%), $FeCl_2$ (Aldrich, 98%), 2-bromopropionitrile (BPN) (Aldrich, 97%), 2-chloropropionitrile (CPN) (Aldrich, 95%), methyl-2-bromopropionate (MBP) (Aldrich, 98%), ethyl 2-bromoisobutyrate (EBriB) (Aldrich, 99%), 1-phenylethyl bromide (PEBr) (Aldrich, 97%),1-phenylethyl chloride (PECl) (TCI, 97%), *p*-xylene (Aldrich, 97%), anisole (Aldrich, 99%), cyclohexanone (Aldrich, 99+%), *N*,*N*-dimethylformamide (DMF) (Aldrich, 99.9+%), diphenyl ether (DPE) (Aldrich, 99%), methyl ethyl ketone (MEK) (Aldrich, 99+%) and all other solvents were used without further purification. The monomers and solvents were purged by bubbling with dry nitrogen for 30 min immediately before polymerization.

2.2. Synthesis of DPPMP

DPPMP was synthesized using the method described by Braunstein and co-workers [29] as follows: a solution of *n*-butyllithium (31.68 mL of a 1.6 M solution in hexane, 50.7 mmol) was added to 2-picoline (4.72 g, 50.7 mmol) in dry THF (20 mL) at −20 °C over a period of 20 min. After stirring (1 h), the mixture was added to a solution of chlorodiphenylphosphine (11.18 g, 50.7 mmol) in dry THF (25 mL) at −60 °C over 30 min, followed by warming to 0 °C over 45 min. The mixture was then cooled to −25 °C and water (50 mL) was added over 10 min, followed by stirring for 30 min. The product was obtained by extraction with an HCl solution (2 × 250 mL, 0.3 M), followed by neutralization with an $NaHCO_3$ solution, and extraction with dichloromethane (3 × 100 mL). The solvent and any unreacted 2-picoline were removed *in vacuo*. The yield of the crude product was 9.7 g (69%). The latter was dissolved in warm EtOH (50 mL) followed by the addition of water (50 mL). Storing overnight at −30 °C gave a cream colored precipitate of the product. This was filtered off and dried *in vacuo*, giving a yield of 8.8 g, 63%. ^{1}H NMR δ 8.50–6.80 (m, C_5H_4N), 8.00–7.00 (m, PC_6H_5), 3.64 (s, CH_2).

2.3. Polymerization procedures

The ATRP of MMA and styrene was carried out using the following procedure: a Schlenk flask was charged with $FeBr_2$ and the ligand. The flask was sealed with a rubber septum and was cycled three times between vacuum and nitrogen to remove the oxygen. The degassed solvent (in solution polymerization) and monomer were then added to the flask through degassed syringes. The solution was stirred for 20 min at room temperature and then the desired amount of initiator was added. The flask was sealed with a new rubber septum and degassed by three freeze–pump–thaw cycles to remove the oxygen. The flask was immersed in a thermostated oil bath. At timed intervals, samples were withdrawn from the flask with a degassed syringe and diluted with THF and then filtered through a column filled with neutral aluminum oxide to remove the iron catalyst. Parts of the polymer solution were used for gas chromatography (GC) measurements in order to determine the monomer conversions. Other parts of the PMMA solution were then precipitated using an excess of *n*-hexane and PS solution was precipitated using an excess of methanol, and these polymers were dried under vacuum for 24 h in preparation for gel permeation chromatography (GPC) measurements to determine the molecular weights of the polymers.

One of the main drawbacks in ATRP is the relative difficulty in removing the colored catalyst residues from the polymers. The catalyst residues change the color of polymers and make them toxic. Therefore, the catalyst residue must be reduced to a low level for most of the applications. In our laboratory, we used three methods to remove the catalyst from the polymers obtained by ATRP. The usual method of removing the catalyst is that polymerization solution is passed though a column containing aluminum oxide. Another method is that polymers are purified by precipitation from acidified methanol solution instead of simply passing through aluminum oxide columns. However, higher $M_{n,GPC}$ values and lower

PDIs were obtained, suggesting that low-molecular weight polymers were soluble in acidified methanol. The third method is the liquid–liquid extraction. The FeX_3 can be extracted from the organic phase to the water phase. Then the purified polymers can be collected after evaporating the solvent.

2.4. Characterizations

^1H (300 MHz) NMR spectra were obtained on a Bruker DPX-300 FT-NMR spectrometer in $CDCl_3$ solvent. The monomer conversion was determined in THF solvent with anisole as an internal standard with an HP 6890 gas chromatograph equipped with an FID detector and a J&W Scientific 30 m DB WAX Megabore column. The injector and detector temperatures were kept at 250 °C. The analysis was run isothermally at 40 °C for 1 min, following which the temperature was increased to 120 °C at a heating rate of 20 °C/min and held at this temperature for 1 min, before being increased again to 180 °C at a heating rate of 10 °C/min and being held at this temperature for 1 min. The number-average molecular weight and molecular weight distribution (M_w/M_n) of the PMMA and PS were determined by GPC using Waters columns (Styragel, HR 5E) equipped with a Waters 515 pump and a Waters 2410 differential refractometer using diphenyl ether as an internal standard. THF was used as the eluent at a flow rate of 1 mL/min. Linear PS standards (1.31×10^3–3.58×10^6 g/mol) were used for calibration.

3. Results and conclusion

It should be noted that there is no need to react the transition metal and the ligand and then isolate the catalyst product. The catalyst composition can directly reacted with the monomer when the FeX_2 and the ligand are in a mixing state. Therefore, the procedures of isolating and purifying the catalyst can be saved and thus the cost is saved. On the second hand, the added aluminum compounds were needed for the metal-catalyzed living radical polymerization using TPP [16,17] as ligand which has a structure similar to that of DPPP. However, FeX_2/pyridylphosphines complexes induced the living radical polymerization of MMA and styrene without use of the aluminum compounds. Moreover, comparison between the catalyst systems $FeBr_2$/DPPP and $FeBr_2$/TPP shows that $FeBr_2$/DPPP gave better control of the polymerization, $M_{n,GPC}$ values were very close to the theoretical line, and low PDIs were observed. On the third hand, high conversions were obtained in relatively short times in the $FeBr_2$/DPPP catalyst system, which indicated an efficient catalyst system. Although the living radical polymerization of MMA polymers was achieved in the above-mentioned studies [16,17], high conversions were obtained only at rather long reaction times. The following results are intended to illustrate the process and the advantages of the FeX_2/DPPP catalyst systems.

The polymerizations of MMA were performed using $FeBr_2$/pyridylphosphines as complex in *p*-xylene (50%, v/v) at 80 °C. Firstly, EBriB was used as initiator because it is one of the most effective and versatile initiators which can be successfully used in the living radical polymerization of MMA [3,22]. The molar ratio of MMA to $FeBr_2$ to ligand to initiator was 200:1:2:1 in the present study. When the pyridylphosphine ligands and $FeBr_2$ were mixed together, the solution turned orange, which is characteristic of the $FeBr_2$/pyridylphosphine complex. During the polymerization of MMA, the color turned garnet after several hours, which indicated the formation of the Fe(III) complex. To demonstrate the advantages of pyridylphosphine ligands, the same experiment was performed with the triphenylphosphine (TPP) ligand. The structure of DPPP is similar to that of TPP, which was used as a ligand in living radical polymerization by Sawamoto and co-workers [16]. The results of the polymerization of MMA with these ligands are shown in Table 1.

It can be seen from Table 1 that the system with DPPP as ligand demonstrated the best controllability among the three ligands. In the case of the polymerization with the $FeBr_2$/TPP catalyst system, the molecular weight was less than the predicted value, and the PDI was high, which indicated that the controllability of the polymerization was poor. Similar results were also obtained in the polymerization of MMA using the $FeCl_2(PPh_3)_2$ catalyst system initiated by CCl_4 or EBriB [16], presumably due to the occurrence of chain-transfer reaction during the polymerization. The PMMA molecular weight with the $FeBr_2$/DPPMP catalyst system was higher than that predicted, indicating the lower efficiency of the initiator system employed in this work. One possible explanation for this behavior is the occurrence of slow initiation with respect to the fast propagation of monomer [12,30,31]. In addition, the molecular weight distributions catalyzed by this system were mostly above 1.5, which indicates that the polymerization can hardly be controlled. Therefore, the $FeBr_2$/DPPP catalyst system was employed in all further experiments.

3.1. Effect of the DPPP-to-$FeBr_2$ molar ratio on the polymerization of MMA

The ligand-to-catalyst molar ratio is a key parameter in the ATRP process, and the amount of ligand must be sufficient for it to form a complex with the catalyst studied in the polymerization medium. These polymerizations of MMA using the $FeBr_2$/DPPP catalyst system initiated by EBriB were carried out in *p*-xylene (50%, v/v) at 80 °C. The results are shown in Table 2. As expected, increasing the DPPP-to-$FeBr_2$ molar ratio led to an enhancement of the polymerization rate. However, in the case of a molar ratio of 2.5:1, the polymerization

Table 1
Effect of ligand on ATRP of MMA at 80 °C[a]

Ligand	Time (h)	Conv (%)	$M_{n,th}$[b]	$M_{n,GPC}$	PDI
DPPP	5	65	13,200	13,100	1.33
DPPMP	4	63	12,900	14,500	1.56
TPP	5	40	4200	3600	1.65

[a] $[MMA]_0 = 4.67$ M; $[MMA]_0/[EBriB]_0/[FeBr_2]_0/[DPPP]_0 = 200:1:1:2$.
[b] $M_{n,th} = ([MMA]_0/[EBriB]_0)M_{MMA} \times Conv\ (\%) + M_{EBriB}$; M_{MMA} and M_{EBriB} are the molecular weights of the monomer, MMA, and the initiator, EBriB.

Table 2
Effect of the ligand-to-catalyst molar ratio on the polymerization of MMA[a]

Entry	$[L]_0/[C]_0$[b]	Time (h)	Conv (%)	$M_{n,GPC}$	PDI	f[c]	k_{app} ($\times 10^{-5}$, s^{-1})
1	1/1	3	47	10,200	1.28	0.94	4.72
2		5	58	12,500	1.33	0.95	
3		8	71	15,900	1.30	0.90	
4	1.5/1	3	50	11,850	1.33	0.86	5.07
5		5	62	14,500	1.33	0.87	
6		8	73	16,300	1.30	0.91	
7	2/1	3	52	10,800	1.32	0.98	6.02
8		5	65	13,100	1.33	1.01	
9		8	81	16,700	1.26	0.98	
10	2.5/1	3	44	9100	1.34	0.98	5.55
11		5	63	12,500	1.43	0.98	
12		8	74	15,900	1.42	0.95	

[a] $[MMA]_0 = 4.67$ M; $[MMA]_0/[EBriB]_0/[FeBr_2]_0 = 200:1:1$.
[b] L = ligand (DPPP); C = catalyst ($FeBr_2$).
[c] $f = M_{n,th}/M_{n,GPC}$.

rate is slightly decreased. Furthermore, in the case of the polymerization with a molar ratio of DPPP to $FeBr_2$ of 2:1, the experimental molecular weights matched the theoretical ones and relatively low molecular weight distributions ($M_w/M_n = 1.25-1.33$) were obtained. However, the molecular weights were higher than that predicted in the case where the molar ratio of DPPP to $FeBr_2$ was 1:1 or 1.5:1. Moreover, in the case where the polymerization was carried out with a molar ratio of 2.5:1, the molecular weight distributions were also broader than those obtained in other molar ratios of DPPP to $FeBr_2$.

Fig. 1 shows the dependence of the apparent rate constant (k_{app}, the slope of $\ln[M]_0/[M]$ vs. time plot) of the polymerization on the [DPPP]:[$FeBr_2$] ratio. The maximum rate constant is observed at a 2:1 ratio of ligand to catalyst. However, the rate of polymerization is slightly decreased in the presence of a higher ligand concentration ([DPPP]:[$FeBr_2$] = 2.5:1). One possible explanation for this is that when the ligand concentration is further increased, the coordination of the ligand to the metal center may hinder the activity of the catalyst, resulting in a slight decrease in the rate of polymerization [11,32].

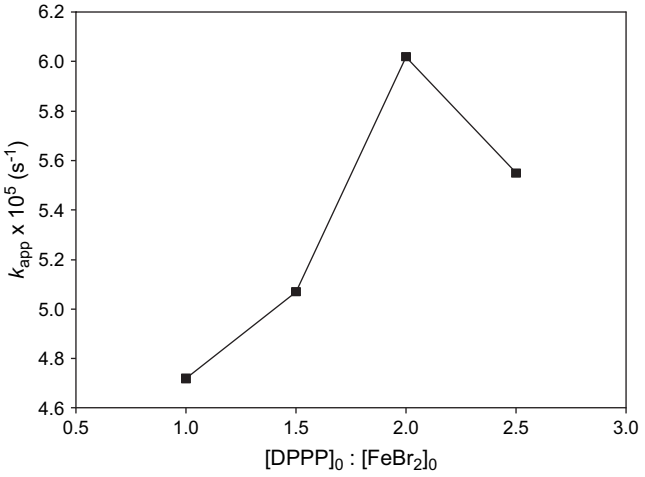

Fig. 1. Plot of k_{app} vs. equivalents of DPPP used for ATRP of MMA using $FeBr_2$/DPPP as catalyst in *p*-xylene at 80 °C. $[MMA]_0 = 4.67$ M; $[MMA]_0/[EBriB]_0/[FeBr_2]_0 = 200:1:1$.

3.2. Effect of the catalyst concentration on the polymerization of MMA

Because of the great importance of the relative amount of catalyst in ATRP processes, various polymerizations of MMA were carried out with different amounts of the catalyst with respect to the initiator in *p*-xylene (50%, v/v) at 80 °C. The initial molar ratio of monomer to initiator was preset at 200, and the DPPP-to-$FeBr_2$ molar ratio was fixed at 2 ($[DPPP]_0/[FeBr_2]_0 = 2:1$) for an initial monomer concentration of 4.67 M. The values of k_{app} and initiation efficiency (f) for the different catalyst concentrations are summarized in Table 3, with f defined as $M_{n,th}/M_{n,GPC}$.

The polymerization rate increased with increasing catalyst concentration. In the case of the higher catalyst concentration ($[C]_0/[I]_0 = 2:1$), a higher rate of polymerization ($k_{app} = 6.94 \times 10^{-5}$ s^{-1}) and initiation efficiency ($f = 0.93$) were obtained, but a broader molecular weight distribution ($M_w/M_n = 1.50$). One possible explanation for these is that the high catalyst concentration, while all other conditions remain unchanged, makes the polymerization medium so viscous that the rate of exchange between the active and dormant species can be changed and, accordingly, the molecular weight distribution will be broadened. On the other hand, in the case of lower catalyst concentration ($[C]_0/[I]_0 = 0.5:1$), a relatively lower rate of polymerization ($k_{app} = 4.07 \times 10^{-5}$ s^{-1}) and lower initiation efficiency ($f = 0.84$) were observed. That may be because, at the low catalyst concentration, even a trace amount of oxygen or other impurities can cause remarkable irreversible chain terminations and other side reactions and thus decrease the catalyst activity and initiation efficiency.

3.3. Effect of initiator on the polymerization of MMA

Fast initiation is required to obtain well-defined polymers with a low PDI [3]. The initiator is thus chosen so that the initiation occurs fast and is quantitative, with the dormant polymer chain end being stable during the polymerization. Therefore, three different initiators were examined for the solution ATRP of MMA, viz. EBriB, BPN and MBP, in conjunction with the $FeBr_2$/DPPP catalyst system in *p*-xylene (50%, v/v) at 80 °C.

Table 3
ATRP of MMA with different catalyst concentrations in *p*-xylene at 80 °C[a]

$[C]_0/[I]_0$	Time (h)	Conv (%)	$M_{n,GPC}$	PDI	f[b]	k_{app} ($\times 10^{-5}$, s^{-1})
0.5	5	53	12,800	1.36	0.84	4.07
1.0	5	65	13,100	1.33	1.01	6.02
1.5	5	68	15,100	1.33	0.91	6.43
2.0	5	70	15,300	1.50	0.93	6.94

[a] $[MMA]_0 = 4.67$ M; $[MMA]_0/[EBriB]_0 = 200:1$; $[FeBr_2]_0/[DPPP]_0 = 1:2$.
[b] $f = M_{n,th}/M_{n,GPC}$.

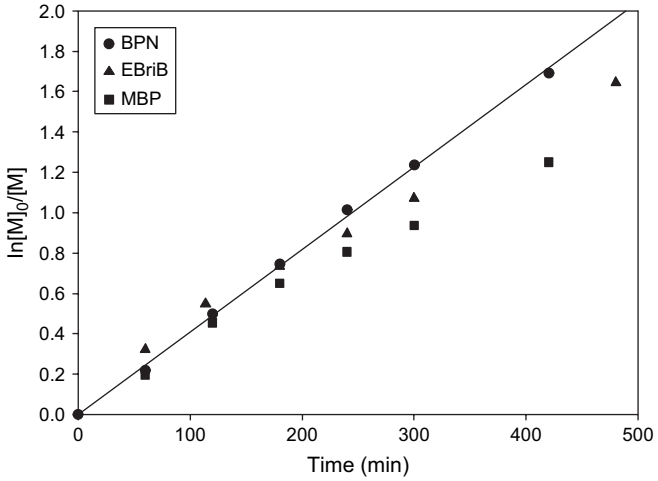

Fig. 2. Kinetic plots of $\ln[M]_0/[M]$ vs. reaction time for the ATRP of MMA in *p*-xylene with different initiators at 80 °C. $[MMA]_0 = 4.67$ M; $[MMA]_0/[initiator]_0/[FeBr_2]_0/[DPPP]_0 = 200:1:1:2$.

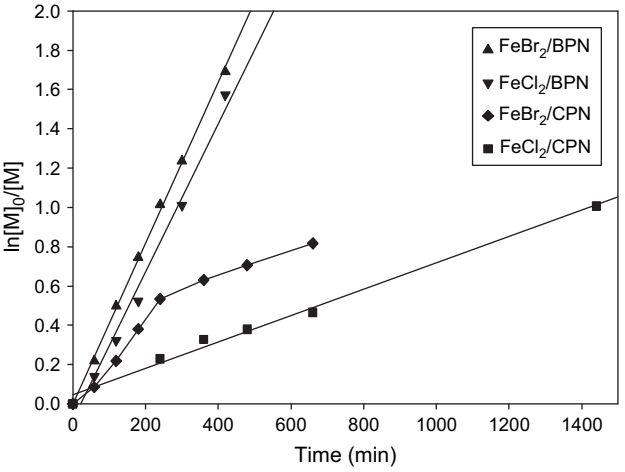

Fig. 4. Kinetic plots of $\ln[M]_0/[M]$ vs. reaction time for the ATRP of MMA in *p*-xylene using FeX_2/XPN initiation systems, where X = Br or Cl at 80 °C. $[MMA]_0 = 4.67$ M; $[MMA]_0/[XPN]_0/[FeX_2]_0/[DPPP]_0 = 200:1:1:2$.

Fig. 2 shows the kinetic plots of the ATRP of MMA with the three initiators. In the EBriB and BPN systems, the $\ln[M]_0/[M]$ data increased linearly with increasing reaction time, which indicated that the radical concentration remained constant during the reactions, whereas the MBP system showed a curvature in the first-order kinetic plots, which indicated that the termination was detectable.

Fig. 3 shows the dependence of M_n and M_w/M_n on the monomer conversion with the different initiators. The experimental molecular weights matched the calculated ones better and the molecular weight distributions ($M_w/M_n = 1.19-1.26$) were narrower when the more active initiator, BPN, was employed instead of EBriB and MBP [10,24]. In the MBP system, the experimental molecular weights were higher than the theoretical line, which was indicative of inefficient initiation caused by slow deactivation. Therefore, BPN was used as the initiator in the following studies.

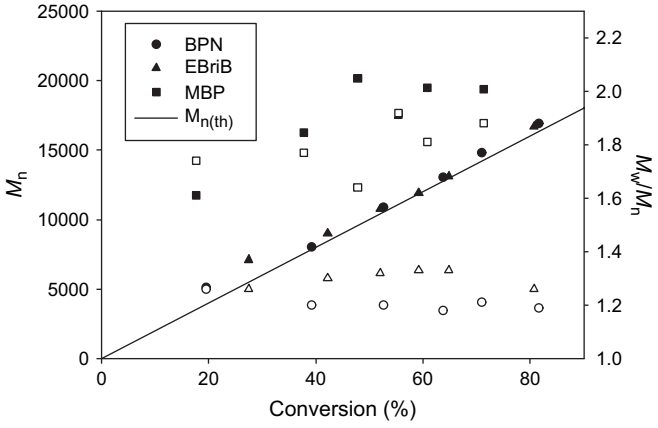

Fig. 3. Dependence of molecular weights, M_n (filled symbols), and molecular weight distributions, M_w/M_n (open symbols), on the monomer conversion for the ATRP of MMA in *p*-xylene with different initiators at 80 °C. $[MMA]_0 = 4.67$ M; $[MMA]_0/[initiator]_0/[FeBr_2]_0/[DPPP]_0 = 200:1:1:2$.

On the other hand, 2-halopropionitriles (XPN, X = Br or Cl) are good initiators for the ATRP polymerization of methacrylates and acrylonitrile. Therefore, the polymerizations of MMA were carried out in *p*-xylene (50%, v/v) at 80°C using the FeX_2/DPPP catalyst system initiated by XPN. All of the experiments described in the present work were conducted using the ratio $[MMA]_0/[XPN]_0/[FeX_2]_0/[DPPP]_0 = 200:1:1:2$. The polymerization of MMA showed first-order kinetics with respect to the monomer for the BPN initiator systems used, as shown in Fig. 4. In the mixed halide initiation systems, $FeCl_2$/BPN gave better control of the polymerization, whereas the $FeBr_2$/CPN initiation system showed a significant curvature in the first-order kinetic plots. A similar polymerization rate was observed when $FeBr_2$/BPN ($k_{app} = 6.82 \times 10^{-5}\ s^{-1}$) or $FeCl_2$/BPN ($k_{app} = 6.32 \times 10^{-5}\ s^{-1}$) was used, but these values were greater than that observed when the polymerization of MMA was carried out using the $FeCl_2$/CPN initiation system ($k_{app} = 1.12 \times 10^{-5}\ s^{-1}$), which was attributed to the strong C–Cl bond. The weakness of the C–Br bond compared with the corresponding C–Cl bond is responsible for the higher rate of polymerization [11,12,33].

Fig. 5 shows the dependence of M_n and M_w/M_n on the monomer conversion with the 2-halopropionitriles as initiation systems. The FeX_2/BPN systems, with their weaker C–Br bond, can generate initiating radicals more efficiently than the FeX_2/CPN systems and yield polymers with molecular weights closer to the theoretical values [34]. The comparison between the initiation systems, $FeBr_2$/BPN and $FeCl_2$/CPN, showed that $FeBr_2$/BPN gave better control of the polymerization, $M_{n,GPC}$ values that were very close to the theoretical line, and low molecular weight distributions ($M_w/M_n = 1.19-1.26$), which indicates that the activation/deactivation process was efficient. However, in the case of the $FeCl_2$/CPN initiation system, the number-average molecular weights were much higher than the theoretical values, which indicated that the efficiency of the initiator systems was low. In the case of the mixed halide initiator systems, $FeCl_2$/BPN gave better control of

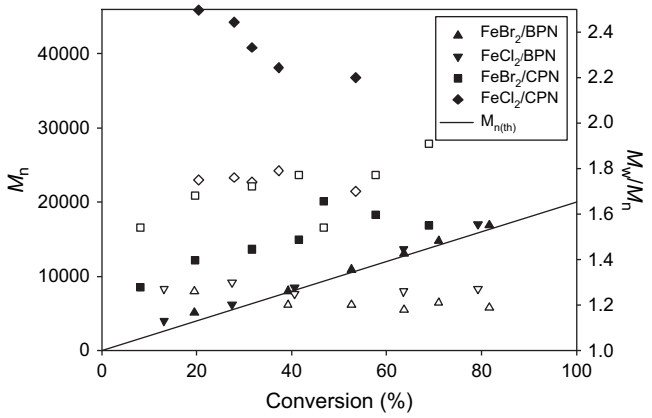

Fig. 5. Dependence of molecular weights, M_n (filled symbols), and molecular weight distributions, M_w/M_n (open symbols), on the monomer conversion for the ATRP of MMA in *p*-xylene using FeX_2/XPN initiation systems, where X = Br or Cl at 80 °C. $[MMA]_0 = 4.67$ M; $[MMA]_0/[XPN]_0/[FeX_2]_0/[DPPP]_0 = 200:1:1:2$.

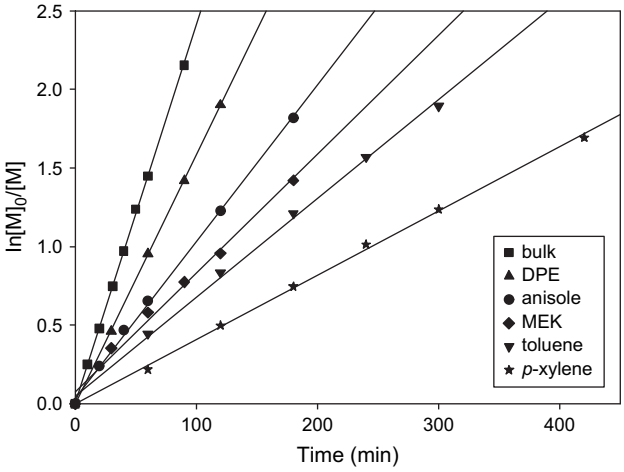

Fig. 7. Kinetic plots of $\ln[M]_0/[M]$ vs. reaction time for the ATRP of MMA in different solvent (50%, v/v) systems at 80 °C. $[MMA]_0 = 4.67$ M; $[MMA]_0/[BPN]_0/[FeBr_2]_0/[DPPP]_0 = 200:1:1:2$.

the polymerization and $M_{n,GPC}$ values which followed the theoretical line, whereas the $FeBr_2$/CPN system gave uncontrolled polymerization, which was attributed to the strong C–Cl bond and inefficient initiation [34].

We also researched the effect of the concentration of the initiator on the polymerization. The polymerizations of MMA catalyzed by $FeBr_2$/DPPP initiated by BPN at three different initiator concentrations were carried out in *p*-xylene (50%, v/v) at 80 °C. The molar ratio of MMA to $FeBr_2$ to DPPP was 200:1:2. The plot of ln k_{app} vs. $\ln[\text{initiator}]_0$ showed the dependence of the polymerization rate on the initiator concentration. As expected, the apparent rate constant of polymerization (k_{app}) increased with increasing initiator concentration. The slope of the line indicated that the rate of polymerization is pseudo order (0.5) with respect to the initiator concentration (see Fig. 6). Thus, a 1:1 ratio of $[FeBr_2]_0/[BPN]_0$ was found to be the optimum ratio for the ATRP of MMA in *p*-xylene at 80 °C.

3.4. Effect of solvent on the polymerization of MMA

As shown in this article, a remarkable solvent effect was observed in the ATRP of MMA initiated by BPN and catalyzed by $FeBr_2$/DPPP. However, to obtain deep insight into the solvent effect, we must compare these data with those obtained in bulk polymerization. Thus, we also tried the bulk polymerization of MMA with $FeBr_2$/DPPP as the catalyst and BPN as initiator. The bulk polymerization of MMA proceeded fast and gave a conversion of 88% after 90 min under the conditions of $[MMA]_0/[BPN]_0/[FeBr_2]_0/[DPPP]_0 = 200:1:1:2$ at 80 °C.

The kinetic curve is presented in Fig. 7. The first-order kinetic with respect to the monomer indicated that the concentration of growing radicals remained constant during the polymerization process. The dependence of M_n and M_w/M_n on the monomer conversion in bulk is shown in Fig. 8. The

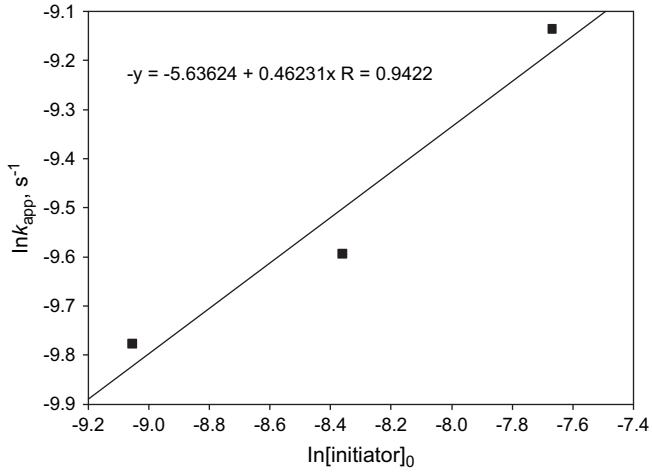

Fig. 6. Dependence of the apparent rate constant of propagation (k_{app}) on the initiator concentration for the ATRP of MMA in *p*-xylene at 80 °C. $[MMA]_0 = 4.67$ M; $[MMA]_0/[FeBr_2]_0/[DPPP]_0 = 200:1:2$.

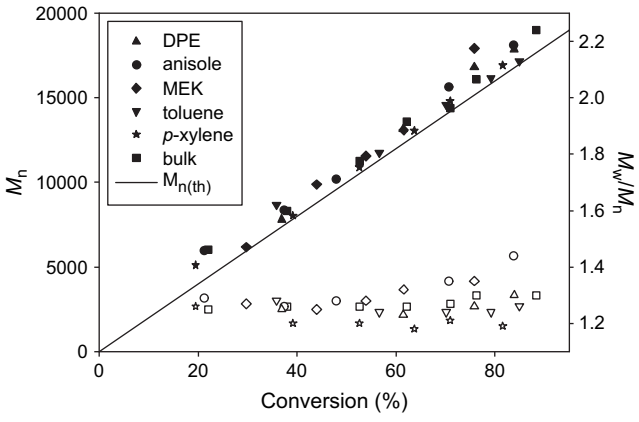

Fig. 8. Dependence of molecular weights, M_n (filled symbols), and molecular weight distributions, M_w/M_n (open symbols), on the monomer conversion for the ATRP of MMA in different solvent (50%, v/v) systems at 80 °C. $[MMA]_0 = 4.67$ M; $[MMA]_0/[BPN]_0/[FeBr_2]_0/[DPPP]_0 = 200:1:1:2$.

experimental molecular weights were higher than the theoretical values, indicating low initiator efficiency. However, the controllability was good in the bulk polymerization, showing a linear increase of M_n with conversion and relatively low polydispersities (PDI = 1.25–1.30). To improve the controllability of the polymerization system, solution polymerization was attempted. Different solvents were investigated for the ATRP of MMA using the $FeBr_2$/DPPP catalyst system initiated by BPN at 80 °C with a monomer concentration of 50% (v/v) for all reactions. The first-order kinetic plots of the polymerizations are shown in Fig. 7. The polymerization rate in the bulk case ($k_{app} = 40.05 \times 10^{-5}\ s^{-1}$) was higher than those obtained from the solution polymerizations due to the reduction of the active radical concentration, the viscosity of the system at the stage of high conversion, and the concentration of the monomer caused by the addition of the solvent [35]. Moreover, in high viscosity systems, the rate of exchange between the active and dormant species can be changed and accordingly, the molecular weight distribution will be broadened.

The polymerization of MMA in DPE proceeded at a much faster rate ($k_{app} = 26.45 \times 10^{-5}\ s^{-1}$) than that in other polar solvents such as anisole ($k_{app} = 16.60 \times 10^{-5}\ s^{-1}$) and MEK ($k_{app} = 12.61 \times 10^{-5}\ s^{-1}$) and nonpolar solvents such as toluene ($k_{app} = 10.50 \times 10^{-5}\ s^{-1}$) and *p*-xylene ($k_{app} = 6.82 \times 10^{-5}\ s^{-1}$). Polar solvents can produce high activity for the ATRP of MMA, because they have the ability to form a homogeneous solution [22]. However, relatively higher M_w/M_n values were observed when anisole and DPE were used as the solvent. Schubert and Zhang [9] also studied the effect of the solvent on the ATRP of MMA catalyzed by $FeBr_2$/*N*-alkyl-2-pyridylmethanimine and found that MEK gave rise to faster polymerization than *p*-xylene, but then a higher reaction temperature was used in MEK.

The dependence of M_n and M_w/M_n on the monomer conversion in different solvents is shown in Fig. 8. The molecular weights of PMMA prepared in all of the solvents increased linearly with increasing monomer conversion. In the cases of the toluene and *p*-xylene solution polymerization systems, the experimental molecular weights followed the theoretical line and narrow polydispersities were observed ($M_w/M_n < 1.3$), whereas in the other polar solvents such as DPE, anisole, and MEK, the $M_{n,GPC}$ values were higher than the predicted ones and slightly higher polydispersities ($M_w/M_n < 1.5$) were observed, which indicated a low initiation efficiency, presumably caused by the slow deactivation.

It is important to study the effect of the concentration of solvent on the reaction system. The results obtained for the ATRP of MMA in various solvents with different concentrations are shown in Table 4. The data obtained for the ATRP of MMA at 80 °C using BPN as initiator and $FeBr_2$/DPPP as catalyst in 33, 50 and 66% (v/v) *p*-xylene solutions are represented. The rate of polymerization in 66% *p*-xylene was slower. The behavior observed when 66% *p*-xylene was used might be due to the reduction of the monomer, initiator and catalyst concentrations, which leads to a decrease in the polymerization rate. The higher experimental molecular weight and relatively higher PDI were observed in the case where 66% *p*-xylene was used, which indicated low initiation efficiency. In the case where 33% *p*-xylene was used, narrow polydispersity (PDI = 1.12) was obtained. Moreover, the efficiency of the polymerization was increased, being significantly higher in 33% *p*-xylene than in 66% *p*-xylene (see Table 4).

Table 4
Effect of solvent on ATRP of MMA with different solvent concentrations[a]

Solvent	Solvent (%, v/v)	Time (h)	Conv (%)	$M_{n,GPC}$	PDI	f[b]	k_{app} ($\times 10^{-5}$, s^{-1})
p-Xylene	33	5	87	18,000	1.12	0.97	10.96
	50	5	82	17,800	1.21	0.97	6.82
	66	5	61	16,000	1.26	0.77	5.19
Toluene	33	3	76	16,500	1.26	0.93	13.29
	50	3	70	14,600	1.24	0.97	10.50
Anisole	33	2	83	18,000	1.34	0.94	21.35
	50	2	71	15,600	1.35	0.92	16.60
MEK	33	3	82	18,300	1.37	0.90	18.26
	50	3	76	17,900	1.35	0.86	12.61
DPE	33	2	85	18,500	1.27	0.91	24.57
	50	2	83	17,800	1.30	0.94	26.45

[a] $[MMA]_0 = 4.67$ M; $[MMA]_0/[BPN]_0/[FeBr_2]_0/[DPPP]_0 = 200:1:1:2$.
[b] $f = M_{n,th}/M_{n,GPC}$.

The polymerizations of MMA were controlled in all of the solvents used in this work. It was remarkable that in the case where 33% (v/v) solvent (*p*-xylene, toluene, anisole and MEK) was used, the k_{app} values were higher than those obtained from the linear part of the kinetic curve when 50% (v/v) of solvent was used in these systems (see Table 4). This behavior is exactly that which would be expected. In the case where 33% solvent was used, the conditions of polymerization are close to those of the bulk reaction and the concentrations of monomer, initiator and catalyst will increase as a result, the polymerization rate should be faster [33,36]. However, a decrease in the amount of DPE (33%, v/v) gave rise to a reduction in the value of k_{app} (see Table 4). One possible explanation for this behavior is that in DPE with its relatively high polarity, the reduction in the amount of solvent will make the polarity of the reaction system decrease, which results in there being a lower concentration of Fe(II) in solution and, consequently the rate of polymerization is reduced [32,37].

3.5. Effect of reaction temperature on the polymerization of MMA

In an effort to gain further mechanistic insights, the effect of the reaction temperature on the polymerization was studied in *p*-xylene (50%, v/v) at 60, 80 and 100 °C.

As shown in Fig. 9, $\ln[M]_0/[M]$ increased linearly with increasing reaction time at all reaction temperatures, suggesting that the radical concentrations in all of these systems were constant. The polymerization rate increased with increasing reaction temperature. Fig. 9 also shows that the polymerization

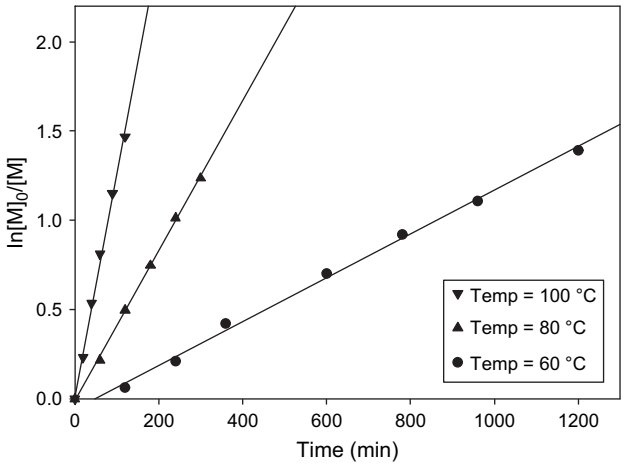

Fig. 9. Kinetic plots of $\ln[M]_0/[M]$ vs. reaction time for the ATRP of MMA in *p*-xylene at different reaction temperatures. $[MMA]_0 = 4.67$ M; $[MMA]_0/[BPN]_0/[FeBr_2]_0/[DPPP]_0 = 200:1:1:2$.

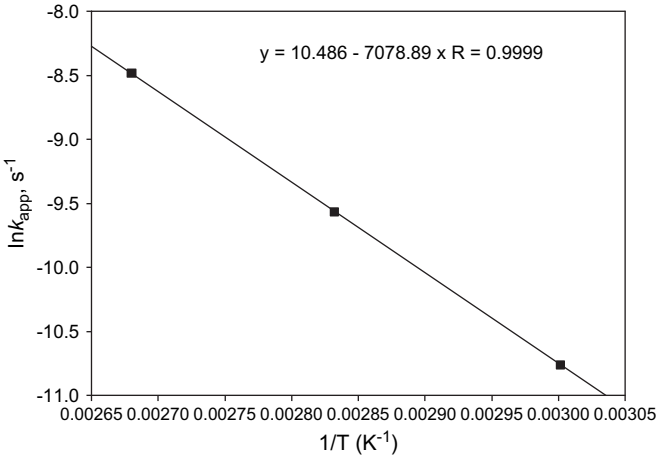

Fig. 11. Plot of $\ln k_{app}$ vs. $1/T$ for the ATRP of MMA initiated by BPN in *p*-xylene. $[MMA]_0 = 4.67$ M; $[MMA]_0/[BPN]_0/[FeBr_2]_0/[DPPP]_0 = 200:1:1:2$.

at lower temperature (60 °C) had a certain induction time. The induction period of the polymerization of MMA was about 60 min for the polymerization at 60 °C. No induction times were observed at 80 and 100 °C. This induction time may be needed for the formation of the $FeBr_2$/DPPP complex.

The effect of temperature on the M_n and M_w/M_n values of the PMMA obtained by ATRP is shown in Fig. 10. The molecular weights of the PMMA prepared at all of the temperatures used herein increased linearly with increasing conversion. They were slightly higher than the theoretical values in the early stage of the reaction, but approached the theoretical values at high conversion, and the initiation efficiencies were above 0.9 at high conversion. The molecular weight distributions were low throughout the polymerization processes. However, those ($M_w/M_n = 1.25–1.32$) of PMMA prepared at 100 °C were slightly higher than those observed at lower temperatures, probably because the thermal acceleration is greater for propagation than for the interconversion rate between the dormant and activated species with temperature [38]. These

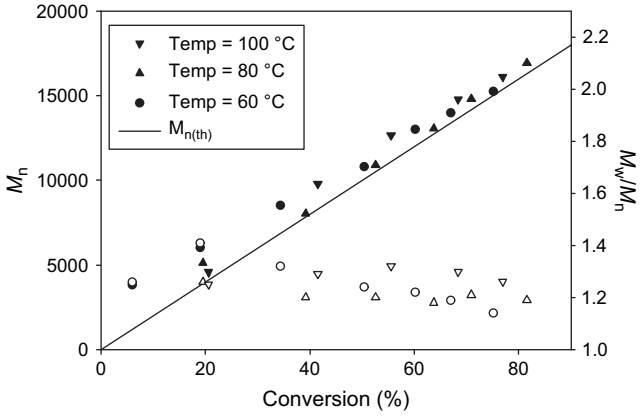

Fig. 10. Dependence of molecular weights, M_n (filled symbols), and molecular weight distributions, M_w/M_n (open symbols), on the monomer conversion for the ATRP of MMA in *p*-xylene at different reaction temperatures. $[MMA]_0 = 4.67$ M; $[MMA]_0/[BPN]_0/[FeBr_2]_0/[DPPP]_0 = 200:1:1:2$.

results indicate that the polymerization of MMA mediated by $FeBr_2$/DPPP proceeded via a living process.

The k_{app} values of the polymerization of MMA at 60, 80 and 100 °C were 2.13×10^{-5}, 6.82×10^{-5}, and 20.72×10^{-5} s^{-1}, respectively. The Arrhenius plot for the $FeBr_2$/DPPP/BPN catalyzed polymerization of MMA is shown in Fig. 11. The apparent activation energy (E_a) calculated for the $FeBr_2$/DPPP/BPN initiation system was 58.9 kJ mol^{-1}. This value was similar to that reported previously by Haddleton et al. [39] for MMA ($E_a = 60.3$ kJ mol^{-1}).

3.6. End-group analysis of PMMA–Br

The end-group analysis of ATRP polymers is important, because polymer chains with halogen end groups act as a macroinitiator. It can be reactivated in the presence of the ATRP catalyst system so as to initiate the polymerization of the second monomer to form block, graft or star polymers, depending on the position and number of initiation sites. In order to check the chain-end functionality of PMMA, the chain extension polymerization of MMA with PMMA–Br ($M_{n,GPC} = 14{,}300$, $M_w/M_n = 1.27$) as macroinitiator to initiate the polymerization of fresh MMA was carried out at 80 °C in *p*-xylene (50%, v/v), using $FeBr_2$/DPPP as the catalyst system. This experiment was conducted using a ratio of $[MMA]_0/[\text{macroinitiator}]_0/[FeBr_2]_0/[DPPP]_0 = 200:0.1:1:2$.

The GPC of the PMMA obtained from this study is shown in Fig. 12. After 4 h, the resulting copolymer showed an increase in its number-average molecular weight ($M_{n,GPC} = 30{,}500$, $M_w/M_n = 1.30$). However, some tailing was observed for the GPC trace of the chain extended polymer. Also, the PDI was slightly higher than that of the macroinitiator, which was likely caused by the slow initiation of the macroinitiator for the chain extension reaction. This chain extension experiment proves that the PMMA obtained by ATRP using BPN as initiator is a living polymer.

An additional method of verifying the functionality of the polymer obtained via ATRP is to analyze the ^1H NMR

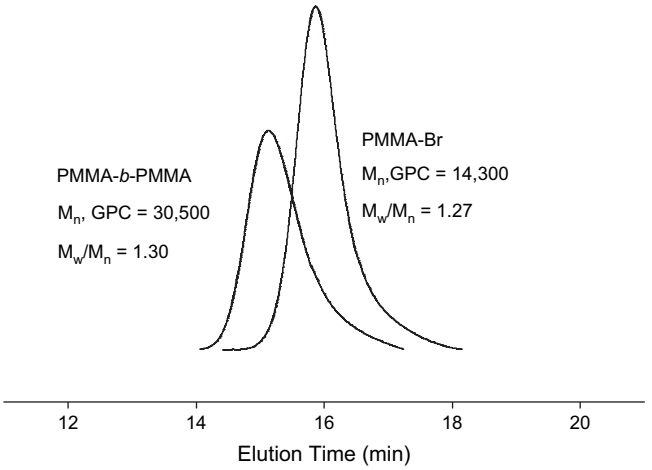

Fig. 12. GPC traces of the macroinitiator (PMMA–Br) and its chain extended polymer (PMMA-*b*-PMMA) obtained at 4 h.

spectrum of the terminal group of the polymer obtained with the BPN/$FeBr_2$/DPPP system. Fig. 13 shows the ^{1}H NMR spectrum of the polymer in $CDCl_3$. As expected, a small signal ($\delta = 3.57$) is observed adjacent to the large methoxy peak ($\delta = 3.82$) of the main chain substituent, which is due to the terminal ester methoxy protons. The number-average molecular weight of the PMMA obtained from the intensity ratio of the peak at $\delta = 3.57$ to that at $\delta = 3.82$, was 20,700, which is in good agreement with the value obtained from GPC ($M_{n,GPC} = 19{,}000$). These results are in agreement with the ones reported by Ibrahim et al. [40,41].

3.7. Polymerization of styrene

$FeBr_2$/pyridylphosphine mediated living radical polymerizations of styrene were performed using PEBr as initiator

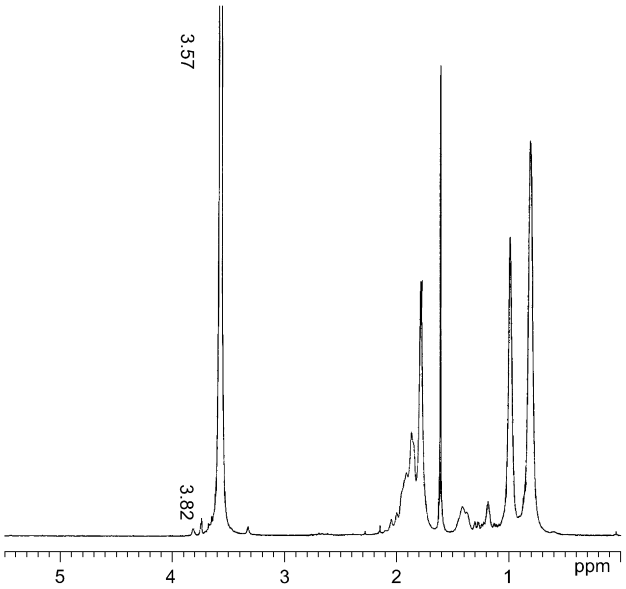

Fig. 13. ^{1}H NMR spectrum (solvent: $CDCl_3$) of the polymer ($M_{n,GPC} = 19{,}000$, $M_w/M_n = 1.30$) prepared via the bulk ATRP of MMA with $[MMA]_0/[BPN]_0/[FeBr_2]_0/[DPPP]_0 = 200:1:1:2$ at 80 °C in 90 min.

Table 5
Effect of ligand on ATRP of styrene at 110 °C[a]

Ligand	Time (h)	Conv (%)	$M_{n,th}$[b]	$M_{n,GPC}$	PDI
DPPP	8	37	3950	5200	1.42
DPPMP	8	49	5300	4200	1.52
TPP[c]	12	40	4300	3800	1.68

[a] $[Styrene]_0 = 8.70$ M; $[styrene]_0/[PEBr]_0/[FeBr_2]_0/[pyridylphosphine]_0 = 100:1:1:2$.
[b] $M_{n,th} = ([styrene]_0/[PEBr]_0)M_{styrene} \times Conv.\ (\%) + M_{PEBr}$; $M_{styrene}$ and M_{PEBr} are the molecular weights of the monomer, styrene and the initiator, PEBr.
[c] $[Styrene]_0/[PEBr]_0/[FeBr_2]_0/[TPP]_0 = 100:1:1:3$.

at 110 °C with a ratio of $[styrene]_0/[PEBr]_0/[FeBr_2]_0/[pyridylphosphine]_0 = 100:1:1:2$. The color of the reaction mixture changed from orange to garnet during the polymerization. The results of the polymerization of styrene with these ligands are shown in Table 5.

The molecular weight of the resulting polystyrene was higher than the theoretical value in the catalyst system consisting of $FeBr_2$/DPPP. One plausible explanation for this is the slow initiation rate induced by the slow activation of the initiator. Moreover, the polydispersity of the polystyrene formed in the reaction was high (PDI = 1.42). However, in the case of the polymerization with $FeBr_2$/TPP and $FeBr_2$/DPPMP, the measured molecular weights were lower than the theoretical values calculated under the assumption that one PEBr initiates one PS chain, and the polydispersities were high (PDI > 1.5), which indicates that the controllability of the polymerizations was poor. A similar phenomenon was observed in the ATRP of styrene with the PEBr/CuBr/bpy initiation system, presumably due to the existence of a chain-transfer process [42].

The results obtained for the ATRP of styrene with different initiation systems are shown in Table 6. The experimental molecular weights were higher than the theoretical ones. This observation may indicate the occurrence of the above-mentioned slow initiation as compared to the fast propagation of the monomer [30,31]. The molecular weight distributions of the PS catalyzed by PECl/$FeCl_2$/DPPP were in the range of

Table 6
Effect of the FeX_2/PEX initiation systems on the polymerization of styrene[a]

Entry	Initiation system	Time (h)	Conv (%)	$M_{n,GPC}$	PDI	f[b]	k_{app} ($\times 10^{-5}$, s^{-1})
1	$FeBr_2$/PEBr	4	26	4700	1.36	0.62	1.58
2		6	31	5100	1.44	0.67	
3		8	37	5200	1.42	0.78	
4	$FeCl_2$/PEBr	4	39	5450	1.27	0.78	2.58
5		6	46	5900	1.44	0.84	
6		8	53	6700	1.45	0.85	
7	$FeBr_2$/PECl	5	34	5700	1.40	0.65	1.94
8		7	42	6100	1.50	0.74	
9		9	47	6200	1.58	0.81	
10	$FeCl_2$/PECl	5	49	6800	1.24	0.77	3.25
11		7	60	7750	1.31	0.82	
12		9	66	8500	1.36	0.83	

[a] $[Styrene]_0 = 8.70$ M; $[styrene]_0/[PEX]_0/[FeX_2]_0/[DPPP]_0 = 100:1:1:2$ (X = Br, Cl).
[b] $f = M_{n,th}/M_{n,GPC}$.

1.2–1.5, which indicates that the polymerization was well controlled. However, the MWDs obtained from the reactions catalyzed by PECl/$FeBr_2$/DPPP were mostly above 1.5, which indicates poor control. In the mixed halide system, the R–Cl bond strength is greater than that of R–Br, and a relative increase in the propagation rate relative to the initiation rate would be expected when using $FeBr_2$, with increased termination and ensuing loss of control [3,43]. The comparison between the initiation systems, PEBr/$FeBr_2$ and PEBr/$FeCl_2$, showed that the latter gave better control of the polymerization, with relatively low polydispersities (PDI = 1.2–1.5) being observed. This result was attributed to the occurrence of side reactions which might have originated from the higher lability of the C–Br bond end group in the PEBr/$FeBr_2$ initiation system. In the mixed initiation system of PEBr/$FeCl_2$, however, most of the PS chains contain a chloride end group, resulting in a decrease in the extent of these side reactions [34,44]. The bulk polymerizations of styrene initiated by PEX and catalyzed by FeX_2/DPPP (X = Cl, Br) have a low initiator efficiency, but exhibit some controlled-radical characteristics, as is evidenced by the linear increase of $M_{n,GPC}$ with increasing conversion, relatively low PDIs and linear first-order rate dependencies for the polymerization reactions.

The polymerizations of styrene using the $FeCl_2$/DPPP catalyst system initiated by PECl were performed in different solvents (50%, v/v) including DMF and cyclohexanone at 110 °C. The first-order kinetic plots of the polymerizations are shown in Fig. 14.

The polymerization of styrene in cyclohexanone medium proceeded at a faster rate than that in DMF, which may be due to the difference in the homogeneity of the reaction system in the different solvents. This result is in good agreement with the report by Zhang et al. [45]. In cyclohexanone, the polymerization proceeded very fast in the beginning of the reaction and then became stabilized, and the dependence of $\ln[M]_0/[M]$ on the polymerization time showed a linear relationship once the polymerization reaction became stable. The linearity of the plot of $\ln[M]_0/[M]$ vs. time in DMF indicated that the polymerization followed first-order kinetic behavior with respect to the monomer concentration and that the concentration of the growing radicals remained constant. In the initiation stage of the polymerization of styrene using cyclohexanone as solvent, the equilibrium between the carbon radicals of the propagation chain and the Fe(III) complex was not yet well established. After the initiation stage, the equilibrium was established and, as a result, the plot of $\ln[M]_0/[M]$ vs. time became linear.

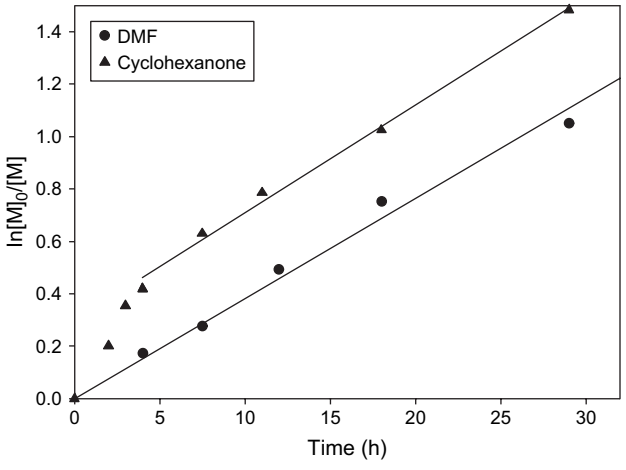

Fig. 14. Kinetic plots of $\ln[M]_0/[M]$ vs. reaction time for the ATRP of styrene in different solvent (50%, v/v) systems at 110 °C. $[Styrene]_0 = 4.35$ M; $[styrene]_0/[PECl]_0/[FeCl_2]_0/[DPPP]_0 = 100:1:1:2$.

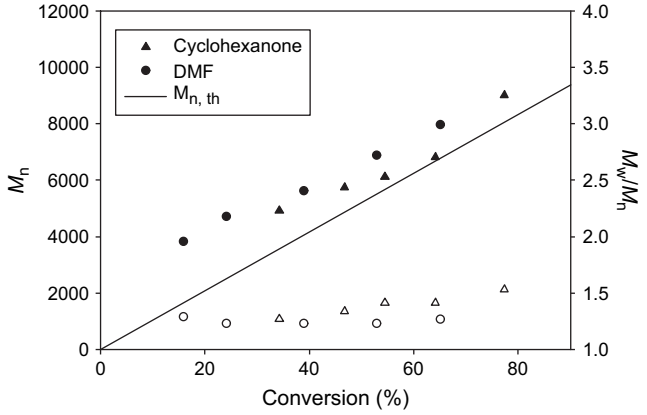

Fig. 15. Dependence of molecular weights, M_n (filled symbols), and molecular weight distributions, M_w/M_n (open symbols), on the monomer conversion for the ATRP of styrene in different solvent (50%, v/v) systems at 110 °C. $[Styrene]_0 = 4.35$ M; $[styrene]_0/[PECl]_0/[FeCl_2]_0/[DPPP]_0 = 100:1:1:2$.

Fig. 15 shows the dependence of M_n and M_w/M_n on the monomer conversion in different solvents. The $M_{n,GPC}$ values of the PS prepared in all of the solvents increased linearly with increasing monomer conversion, but were higher than the theoretical ones. In the case of the polymerization using DMF as solvent, low PDIs (1.2–1.3) were obtained, which indicates that chain transfer and termination did not occur obviously during the period of polymerization. However, slightly higher PDIs (1.2–1.5) were observed in cyclohexanone. All these results indicated that DMF was the better solvent for the ATRP of styrene using $FeCl_2$/DPPP catalytic system.

4. Conclusions

The pyridylphosphine ligand, DPPP, was successfully employed in the ATRP of MMA and styrene. In the $FeBr_2$ mediated ATRP of MMA, the optimum conditions for the DPPP ligand were found to be 200:1:1:2 ($[MMA]_0/[EBriB]_0/[FeBr_2]_0/[DPPP]_0$) ratio in *p*-xylene (50%, v/v) at 80 °C, which yielded a well-defined PMMA with a narrow molecular weight distribution. BPN showed better control of the polymerization reaction with faster initiation and slower propagation. The bulk and *p*-xylene solution polymerizations showed better control of the polymerization of MMA initiated by the BPN/$FeBr_2$/DPPP system, with quite narrow PDIs being obtained. The apparent activation energy of the MMA polymerization catalyzed by $FeBr_2$/DPPP with BPN as initiator was 58.9 kJ mol^{-1}. The controlled nature of the polymerization was confirmed by the formation of high molecular weight

PMMA ($M_{n,GPC} = 30{,}500$, $M_w/M_n = 1.30$) using a PMMA macroinitiator in a chain extension experiment. The ATRP of styrene was successfully performed using PEX as initiator and FeX_2/DPPP as catalyst in the case of the bulk polymerization (X = Cl, Br). The polymerization of styrene can be well controlled in the solvent of DMF.

Acknowledgement

We are grateful to the Korea Science and Engineering Foundation (R01-2004-000-10563-0) for the financial support and the BK21 program for support of Mr. Xue.

References

[1] Patten TE, Matyjaszewski K. Acc Chem Res 1999;32(10):895–903.
[2] Patten TE, Matyjaszewski K. Adv Mater 1998;10(12):901–15.
[3] Matyjaszewski K, Xia J. Chem Rev 2001;101(9):2921–90.
[4] Cheng ZP, Zhu XL, Kang ET, Neoh KG. Langmuir 2005;21(16):7180–5.
[5] Krishnan R, Srinivasan KSV. Macromolecules 2003;36(6):1769–71.
[6] Matyjaszewski K, Wang J. J Am Chem Soc 1995;117(20):5614–5.
[7] Chen J, Chu J, Zhang K. Polymer 2004;45(1):151–5.
[8] Zhang H, Van der Linde R. J Polym Sci Part A Polym Chem 2002; 40(21):3549–61.
[9] Zhang H, Schubert US. J Polym Sci Part A Polym Chem 2004;42(19): 4882–94.
[10] Matyjaszewski K, Wei M, Xia J, Mcdermott NE. Macromolecules 1997; 30(26):8161–4.
[11] Krishnan R, Srinivasan KSV. Macromolecules 2004;37(10):3614–22.
[12] Wang JL, Grimaud T, Shipp DA, Matyjaszewski K. Macromolecules 1998;31(5):1527–34.
[13] Carlmark A, Vestberg R, Jonsson EM. Polymer 2002;43(15):4237–42.
[14] Wang JS, Matyjaszewski K. Macromolecules 1995;28(23):7901–10.
[15] Raghunadh V, Baskaran D, Sivaram S. Polymer 2004;45(10):3149–55.
[16] Ando T, Kamigaito M, Sawamoto M. Macromolecules 1997;30(16): 4507–10.
[17] Kato M, Kamigaito M, Sawamoto M, Higashimura T. Macromolecules 1995;28(5):1721–3.
[18] O'Reilly RK, Gibson VC, White AJP, Williams DJ. J Am Chem Soc 2003;125(28):8450–1.
[19] Zhu S, Yan D. Macromolecules 2000;33(22):8233–8.
[20] Schubert US, Eschbaumer C, Heller M. Org Lett 2000;2(21):3373–6.
[21] Cheng Z, Zhu X, Chen M, Chen J, Zhang L. Polymer 2003;44(8): 2243–7.
[22] Nanda AK, Matyjaszewski K. Macromolecules 2003;36(5):1487–93.
[23] Amass AJ, Wyres CA, Colclough E, Hohn IM. Polymer 2000;41(5): 1697–702.
[24] Göbelt B, Matyjaszewski K. Macromol Chem Phys 2000;201(14): 1619–24.
[25] Gibson VC, O'Reilly RK, Wass DF. Polym Prep 2002;43:167–8.
[26] Gibson VC, O'Reilly RK, Reed W, Wass DF, White AJP, Williams DJ. Chem Commun 2002;17:1850–1.
[27] Matyjaszewski K. Macromol Symp 2002;182(1):209–24.
[28] Newkome GR. Chem Rev 1993;93(6):2067–89.
[29] Braunstein P, Heaton BT, Jacob C, Manzi L, Morise X. Dalton Trans 2003;7:1396–401.
[30] Sumerlin BS, Neugebauer D, Matyjaszewski K. Macromolecules 2005; 38(3):702–8.
[31] Li M, Min K, Matyjaszewski K. Macromolecules 2004;37(6):2106–12.
[32] Mittal A, Sivaram S. J Polym Sci Part A Polym Chem 2005;43(21): 4996–5008.
[33] De la Fuente JL, Fernández-Sanz M, Fernández-García M, Madruga EL. Macromol Chem Phys 2001;202(12):2565–71.
[34] Matyjaszewski K, Shipp DA, Wang JL, Grimaud T, Patten TE. Macromolecules 1998;31(20):6836–40.
[35] Chu J, Chen J, Zhang K. J Polym Sci Part A Polym Chem 2004;42(8): 1963–9.
[36] Matyjaszewski K, Patten TE, Xia J. J Am Chem Soc 1997;119(4): 674–80.
[37] Matyjaszewski K, Nakagawa Y, Jasieczek CB. Macromolecules 1998; 31(5):1535–41.
[38] Uegaki H, Kotani Y, Kamigaito M, Sawamoto M. Macromolecules 1998; 31(20):6756–61.
[39] Haddleton DM, Kukulj D, Duncalf DJ, Heming AM, Shooter AJ. Macromolecules 1998;31(16):5201–5.
[40] Ibrahim K, Yliheikkilä K, Abu-Surrah A, Löfgren B, Lappalainen K, Leskelä M, et al. Eur Polym J 2004;40(6):1095–104.
[41] Ibrahim K, Starck P, Löfgren B, Seppälä J. J Polym Sci Part A Polym Chem 2005;43(21):5049–61.
[42] Qiu J, Matyjaszewski K. Macromolecules 1997;30(19):5643–8.
[43] Xu Y, Lu J, Xu Q, Wang L. Eur Polym J 2005;41(10):2422–7.
[44] Matyjaszewski K, Teodorescu M, Miller PJ, Peterson ML. J Polym Sci Part A Polym Chem 2000;38(13):2440–8.
[45] Zhang W, Zhu X, Zhu J, Chen J. J Polym Sci Part A Polym Chem 2006; 44(1):32–41.